Experimental study of local and integral efficiency behavior of a concave holographic diffraction grating

E. G. Loewen

Milton Roy Company, Analytical Products Division, 820 Linden Avenue, Rochester, New York 14625

E. K. Popov and L. V. Tsonev

Bulgarian Academy of Sciences, Institute of Solid State Physics, 72 Lenin Boulevard, BG-1784 Sofia, Bulgaria

J. Hoose

Milton Roy Company, Analytical Products Division, 820 Linden Avenue, Rochester, New York 14625

Received November 9, 1989; accepted April 17, 1990

It has long been observed that the efficiency behavior of concave gratings differs from that of the well-studied plane gratings. In particular, peak values are less, and anomalies are usually absent or at least greatly attenuated. A detailed study of a typical holographic grating shows how variations in behavior over its surface combine in producing these results.

INTRODUCTION

Many investigations, starting with a paper of H. A. Rowland in 1882, have been devoted to the geometrical focal properties of concave gratings with different blank and groove shapes.[1–3] However, detailed studies of their spectral efficiency behavior (i.e., the distribution of local efficiency over the grating surface and connection of this distribution with total, or integral, efficiency, as well as comparisons between experimental and theoretical evaluation of concave grating efficiency in a given spectral region) have appeared only recently.[4–6] Probably, the main reason for this fact is not due to experimental difficulties but rather to the lack of a well-developed theory of gratings with arbitrary period, modulation, and groove profile. Without such a theory, and its appropriate computer code, it is impossible to carry out the above-mentioned studies, to analyze the experimental data, and to make sufficiently valid conclusions. Indeed, we have gained access to such a theory and computer codes only in the past decade.[7,8]

Compared with plane gratings, the imaging and efficiency behavior of concave gratings is considerably more complex. Rather than being illuminated by a uniform beam of collimated light, they usually receive light from a conical beam, which may or may not be uniform. Except in the meridional plane, the imaging rays will be skewed, so that simple diffraction-efficiency theory should be replaced by the conical version for such calculations. However, because groove depth modulation tends to be low in most concave gratings, the effect of nonuniform groove geometry turns out to be the most important factor, by far, for efficiency considerations.

In the case of mechanically ruled concave gratings, the geometrical characteristic that varies across the grating area is the blaze angle. This is the inevitable result of the interaction of a tool that has a fixed slope angle with a blank whose curvature changes progressively. For low blaze angles, this led to the introduction of bipartite or tripartite rulings, in which the ruling process is interrupted once or twice in order to readjust the diamond tool angle. Otherwise, the ruled area would be restricted to an undesirably small size.[6]

In the case of so-called holographic gratings, which are generated by coherent light emanating from two appropriately located pinholes, the typically Gaussian distribution of such beams will tend to overexpose the center and underexpose near the edges of the resist coated blank. This can result in significant nonuniformity of groove depth in the radial direction.

With each ray undergoing a different angular path and interacting with a groove of different geometry, it is clear that some form of efficiency averaging must take place at the imaging plane. The long-observed result is that integral efficiency peaks are reduced, compared with plane gratings, in return for which the spectral region of reasonable efficiency is broadened. The other observation is that anomalous changes in efficiency virtually disappear, since they are associated with narrowly defined angles of incidence and diffraction.

Hunter and Nevière[4,5] investigated both experimentally and theoretically the distribution of local diffraction efficiency across a concave grating, the so-called efficiency map. They worked only in the vacuum-ultraviolet region, 200–1600 (Ref. 4) or 160–2550 Å (Ref. 5), at normal and grazing incidences and at intermediate angles.

Classically ruled, holographic blazed, and sinusoidal concave gratings with a period d of 1.667 or 0.833 μm are compared. The wavelength-to-period ratio λ/d lies in the interval 0.009–0.3. In this domain grating diffraction is virtually

0740-3232/90/091764-06$02.00

free of polarization effects, including anomalies, and therefore lends itself to much simpler scalar-type analysis.[6,9] That is why all the data in Refs. 4 and 5 are given for unpolarized light. The gratings used had low modulation, the groove-depth-to-period ratio h/d was less than 0.1.[2] To obtain the total efficiency as a function of wavelength, Hunter and Nevière showed the average value of the relevant efficiency map.[4–6]

The main conclusions of Hunter and Nevière were that (i) local efficiency distribution of holographic blazed concave gratings is much more uniform than for conventional plane ruled gratings; (ii) concave blazed ruled or holographic ratings do not have a completely uniform efficiency map primarily because of the change in blaze angle across the surface; (iii) the electromagnetic theory of gratings in its present-day state, e.g., Refs. 7 and 8, can produce accurate efficiency maps for both TE and TM polarization, at least for shallow grooves.

In the present paper we concentrate only on a holographic quasi-sinusoidal grating designed for a color-measuring spectrograph. It is coated with aluminum, has a 100-mm diameter, a 211-mm radius of curvature, and a 793-grooves/mm frequency and is designed to produce a flat field spectrum, over the wavelength range 380–780 nm, for use in a spectrograph with near-normal incidence and imaging. The choice of an $F/2$ aperture for the grating was made not so much to enhance throughput (entendue) but to capture the entire input cone of light. Failure to do so would enhance stray light, a key concern in color measurement. In the spectral region mentioned λ/d varies over a range of 0.30–0.62, i.e., outside the scalar domain, and therefore we can expect anomalies and a different behavior of TE and TM polarizations (in the vacuum ultraviolet we would have 100 nm/1250 nm = 0.08, i.e., scalar conditions). This fact places exacting demands on the theoretical approach and computer codes required for data analysis. In addition, we apply a flexible-averaging procedure for calculating the integral (total) efficiency, and we present complete efficiency maps in meridional and sagittal directions at different wavelengths.

GROOVE-DEPTH DISTRIBUTION

In the absence of good direct methods for groove-depth measurement, an indirect one that has proven effective in the past was chosen. It consists of measuring the Littrow-mount absolute first-order diffraction efficiency (in our case at 632.8 nm) in both TM and TE planes of polarization (for which the electric field vector is perpendicular or parallel to the grooves, respectively). Additional redundant data for cross-checking are readily obtained by repeating the measurements under normal incidence conditions. Data were taken over a network of 69 points on a 1-cm × 1-cm-grid network with the aid of a removable plastic target screen placed over the grating. Its center coincides with the grating pole, the axes being parallel and perpendicular to the grooves.

Experimental data were correlated with theoretical values that are calculated as a function of h/d, provided that one can assume only a sinusoidal groove shape. Any lack of symmetry in shape is readily discerned by comparing positive with negative first-order efficiencies under normal incidence. The final result, in the form of a three-dimensional map, is shown in Fig. 1. It is evident that modulation ranges from a central maximum of 15.9% (considered intermediate) to 4.2% near the edges (i.e., very low), a ratio of almost 4:1.

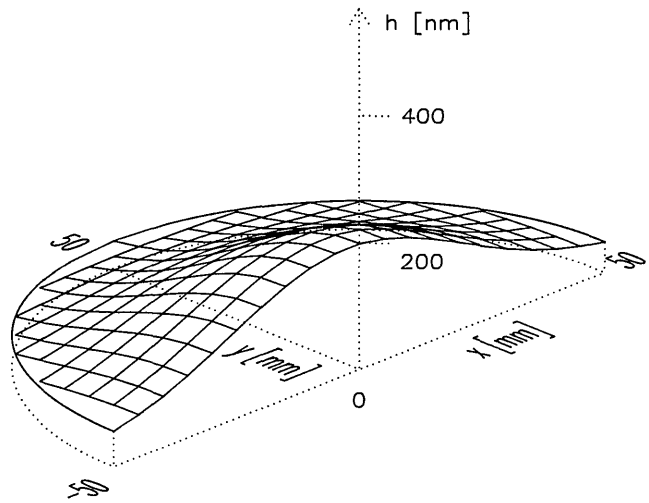

Fig. 1. Three-dimensional map of groove-depth distribution.

LOCAL EFFICIENCY DISTRIBUTION

The next step was to obtain experimental local efficiency maps at different wavelengths in both TM and TE polarizations at each of the same 1-cm × 1-cm-grid network points. Lasers provide the high-intensity small beam size required (1.5-mm diameter at the $1/e$ intensity level), together with excellent polarization control and knowledge of exact wavelength. A two-axis steering mirror serves to direct the beam to each of the 69 points. Such conical sets of fine beams simulate the detailed structure of global grating illumination through an entrance pinhole. The solid-state detector used needs merely to move sideways if the wavelength changes (Fig. 2). Five different lasers, operated at 10 different wavelengths, provide nearly complete wavelength coverage to characterize the behavior. They were He–Cd (441.6 nm), Ar^+ (476 and 514.5 nm), He–Ne (632.8 nm), Kr^+ (647.1 and 676.4 nm), and a dye laser to cover the intermediate region (570, 590, 600, and 620 nm).

Representative results are shown in Fig. 3, in which efficiency at each of the most significant wavelengths in TM and TE planes is plotted as a function of X for the values of Y indicated; the axes are perpendicular and parallel to the grating grooves, respectively, for X and Y. Only positive values for Y are included since corresponding ones for negative values differ by negligible amounts. Efficiency distribution is not uniform, but in our case this has nothing to do with blaze effects, as they did in Ref. 5.

The effect that groove modulation has on the efficiency is clearly visible. At 441.6 nm, the central modulation of 15.9% is too great for maximum efficiency, while at the edges the modulation is too low. Optimum modulation for the blue region appears to be 13.2% (i.e., where X or Y are near 20 mm and for which an absolute efficiency of 32% is ob-

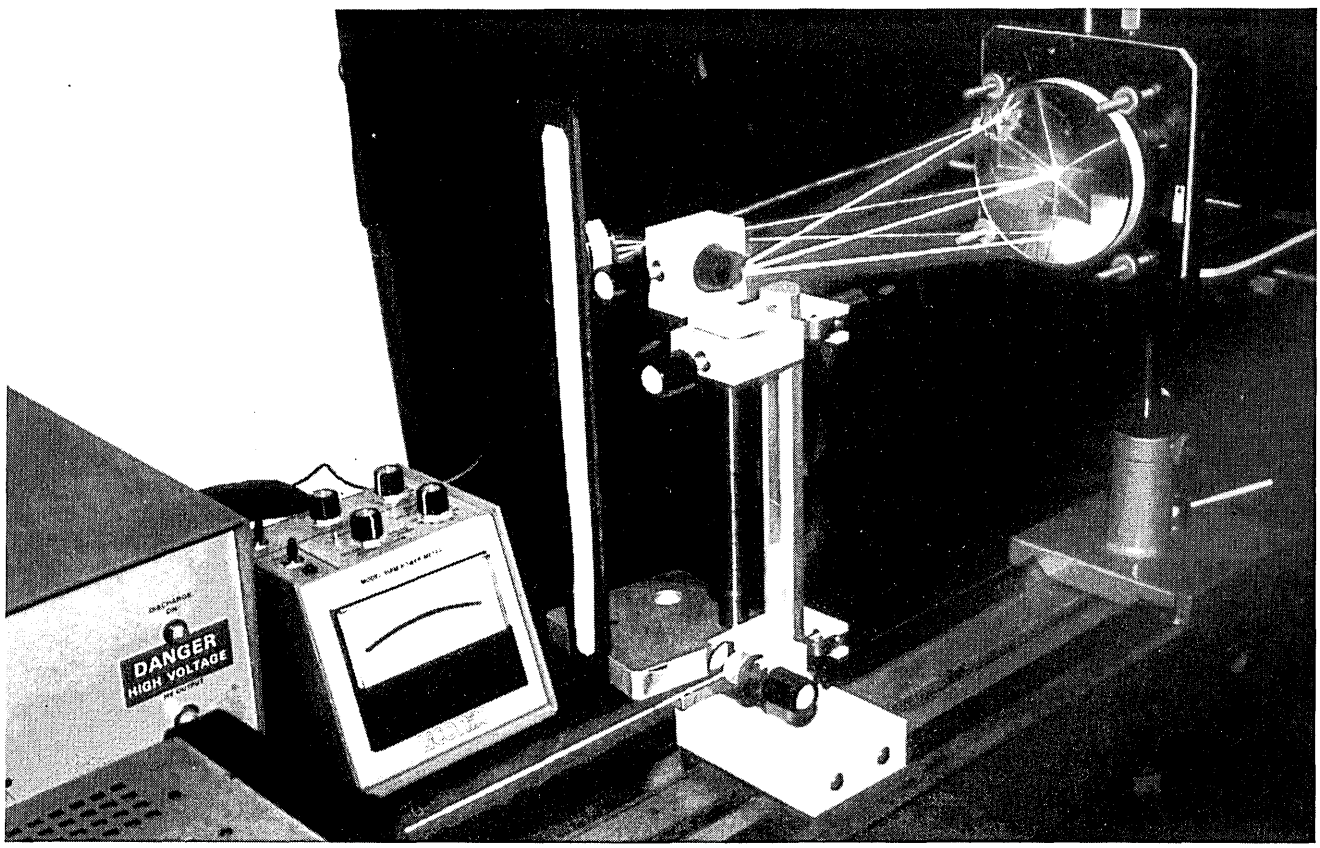

Fig. 2. Experimental setup for local efficiency measurement.

served), which is just 2% less than the theoretical peak for scalar diffraction of infinite conductors.

At 600 nm, no dips occur because, at $\lambda/d = 0.475$, there are no anomalies in this depth-modulation region and this particular deviation from Littrow mount and because the peak efficiency occurs only approximately 10 mm from the grating center.

The picture changes significantly at 676.4 nm because, with λ/d increasing to 0.538, there is an anomaly in TM polarization that is so sharp that it disappears only if $Y = 40$ mm, i.e., if the modulation becomes less than 5%.

It is evident that (in contrast to Ref. 4) local efficiency changes along the sagittal diameter (along Y) as much as it does along the meridional one (along X). The variations in both directions are comparable with each other; therefore a single meridional scan is not enough for correct presentation of an efficiency map.

The nonuniformity of the efficiency maps gives us an excellent opportunity for checking the local efficiency against computer codes, which include the effect of the aluminum surface and its thin oxide layer but assume perfect sinusoidal groove form. The results for the same three wavelengths and both polarizations, taken in the meridional plane, are shown in Fig. 4. The agreement is excellent, not only on the meridional diameter presented here but all over the grating area. It enables us to make some important conclusions:

(i) The assumption of a sinusoidal groove profile seems to be correct.

(ii) For h/d of as much as 0.16, i.e., even for intermediate modulation, Nevière's approach that a concave grating can be treated theoretically by approximating it with an appropriate set of small tangential plane gratings is confirmed.

(iii) It is possible to calculate the efficiency map of a concave grating with high accuracy not only in the vacuum ultraviolet[5] but in the visible spectral region too (assuming that the profile and the depth distribution of the grooves are known).

SPECTRAL BEHAVIOR AND ILLUMINATION OF THE GRATING

After local characteristics are determined with good accuracy, we can examine the behavior of the grating if it is illuminated by a conical beam with a specified transverse energy distribution. This can be done by summing the local efficiencies of the above-mentioned 69 rays at each of the wavelengths of interest, but each local efficiency must be multiplied by a weighting coefficient expressing the relative local intensity of the incident beam at that point.

In classical instruments, the grating is illuminated through an entrance slit; light comes from a lamp through a series of mirrors. In such cases the transversal intensity distribution of the incident beam is remarkably uniform for all practical purposes. Direct total spectral measurements of the grating were performed with an efficiency tester that simulates grating illumination in a typical spectrograph. Input is from a multimode silica fiber that obtains its input from a small monochromator. Two masks, with 9-mm and

32-mm diameters are used to observe both local and integrated behavior in a wide spectral domain.

Figure 5 contains a set of TM and TE spectral efficiency dependences with successive apertures of 9, 32, and 100 mm. They clearly demonstrate the progressive attenuation and the final disappearance of anomalies as the F number decreases, despite the relatively low local efficiencies near the edge of the grating.

In Fig. 6, directly measured, total $F/2.1$ spectral dependence (solid curve) is compared with locally measured and then integrated efficiency values for a homogeneous incident beam (dotted curve). The coincidence is good. The result is the same if local values are not measured but theoretically predicted.

It is interesting also to examine grating behavior under inhomogeneous illumination. As a convenient approximation, the illuminating beam is taken to be Gaussian (Fig. 7) for which ϕ_G is the angle subtended by the grating. In practice if fibers are used for illumination, the field could be Gaussian if the input is properly adjusted. The ratio ϕ_B/ϕ_G can be varied by controlling the F number at the fiber input, i.e., the distance to the lamp filament. F number can easily go from 0.2 to 1, but a normal goal is to aim for 0.5, meaning that $\phi_B/\phi_G = 1$ for the grating that we are considering. The reason is that we want no light to extend outside the grating

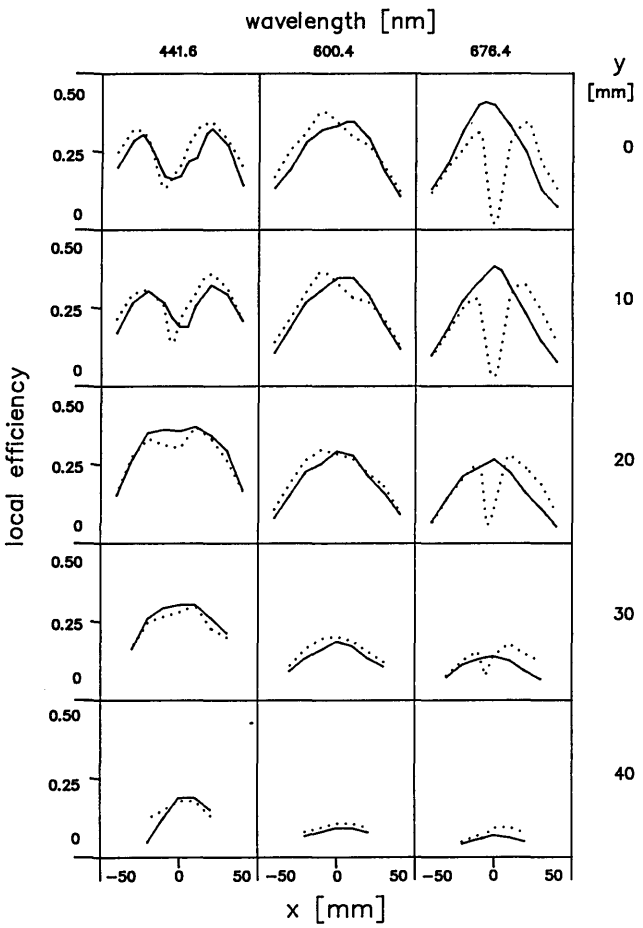

Fig. 3. Local absolute efficiency maps measured at three wavelengths: solid curve, P (or TE); dotted curve, S (or TM) polarization.

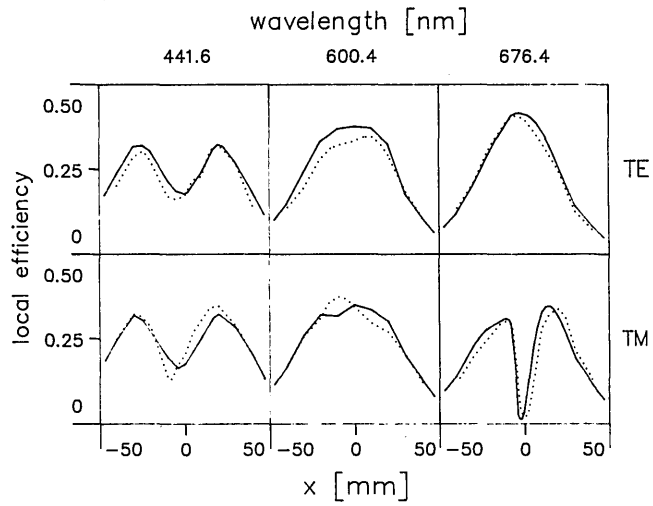

Fig. 4. Comparison between experimental data (dotted curve) and theoretical calculations (solid curve) of local absolute efficiency along the meridional diameter ($y = 0$) for P (TE) and S (TM) polarizations.

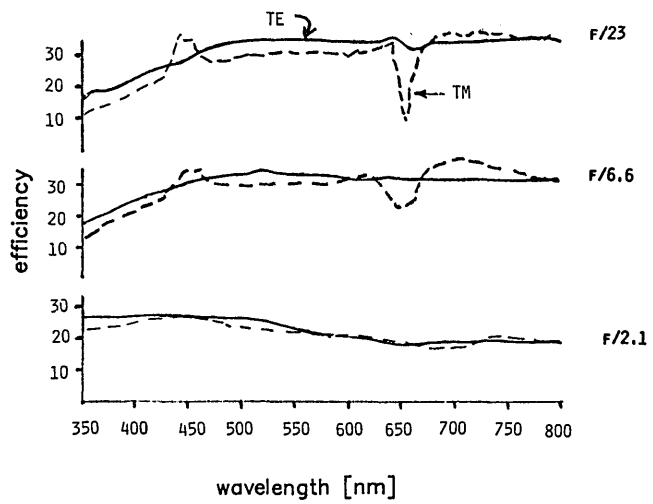

Fig. 5. Efficiency curves for various $F/\#$'s of the same grating show the measured total relative efficiency versus wavelength through different grating apertures for TE and TM polarizations.

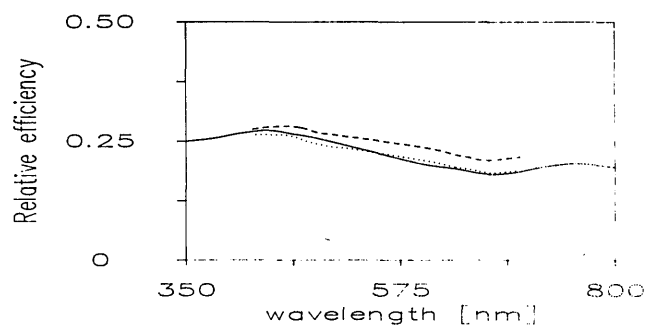

Fig. 6. Measured relative spectral dependence for unpolarized light with $F/2.1$ (solid curve) compared with integrated data calculated for uniform illumination (dotted curve) and for Gaussian illumination with $\phi_B/\phi_G = 1$ (dashed curve).

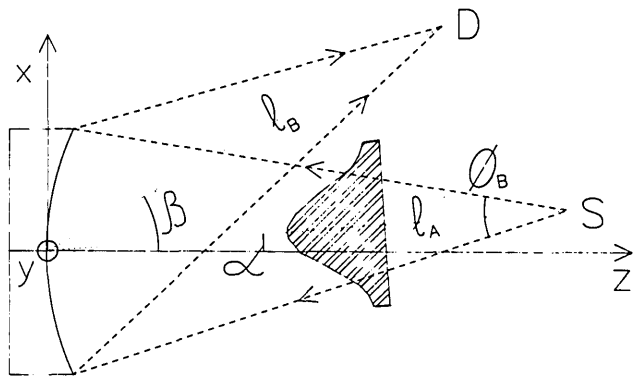

Fig. 7. Beam geometry: S, source; D, detector; α and β, angles of incidence and of diffraction; ϕ_B, effective angular width of the incident Gaussian beam at $1/e$ intensity level.

diameter, not because efficiency is a consideration but because to do so invites extra stray light to reach the detector. Total absolute efficiency is shown in Fig. 8 in the TM and TE planes as a function of ϕ_B/ϕ_G for the same three wavelengths as in Fig. 4. For reasonable values of this ratio, i.e., for $0.5 < \phi_B/\phi_G < 1$, there is remarkably little difference between the three cases. If the illumination is concentrated in the center of the grating (i.e., if $\phi_B/\phi_G = 0.2$), significant effects of wavelength can now be expected. At 441 nm the total efficiency will be reduced, at 600 nm it will be increased, and at 676 nm polarization becomes prominent. There is an optimum for $\phi_B/\phi_G = 0.3$ from an efficiency point of view. The integrated relative efficiency at Gaussian illumination with $\phi_B/\phi_G = 1$ is presented for comparison (dashed curve with in Fig. 6). The small decrease of flat illumination values with respect to Gaussian illumination values is a natural consequence of relatively high energy flow

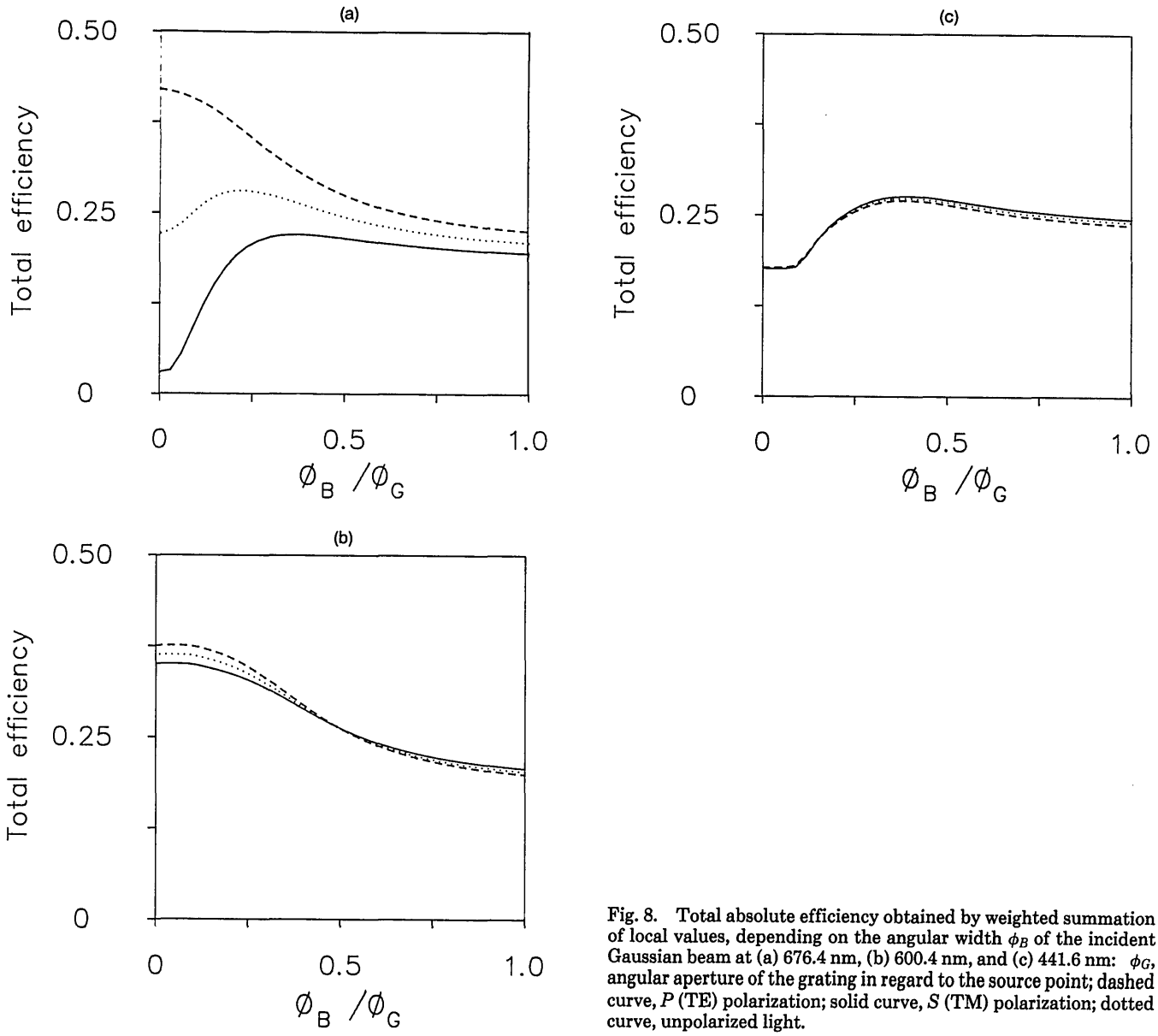

Fig. 8. Total absolute efficiency obtained by weighted summation of local values, depending on the angular width ϕ_B of the incident Gaussian beam at (a) 676.4 nm, (b) 600.4 nm, and (c) 441.6 nm: ϕ_G, angular aperture of the grating in regard to the source point; dashed curve, P (TE) polarization; solid curve, S (TM) polarization; dotted curve, unpolarized light.

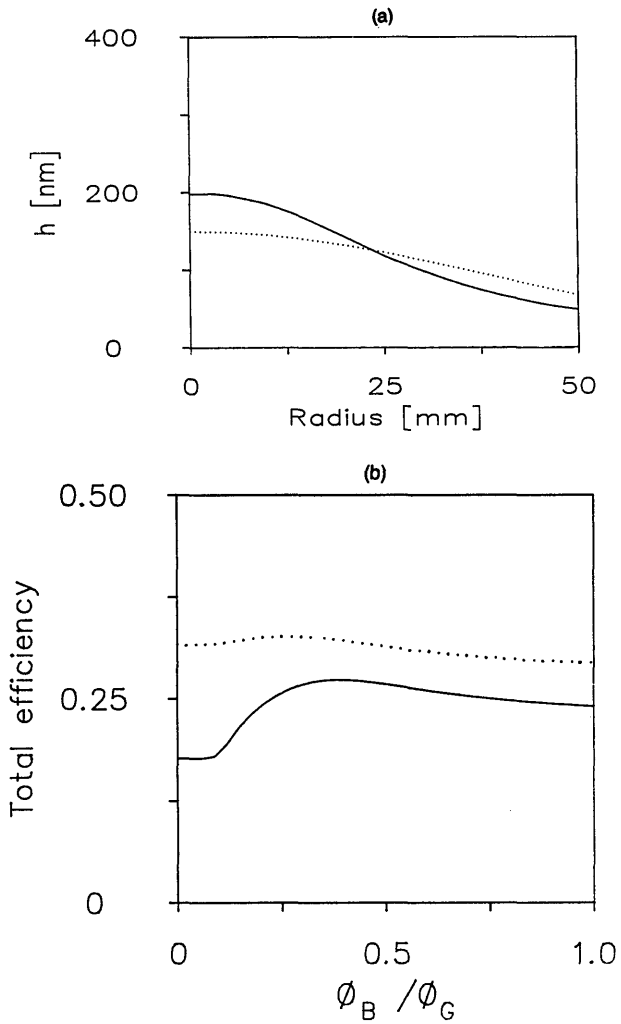

Fig. 9. (a) Radial groove-depth distribution: actual (solid curve) and optimized (dotted curve) (from Fig. 1). (b) Total absolute efficiency versus incident beam angular width ϕ_B in unpolarized light at 441.6 nm for the actual groove-depth distribution (solid curve) and for the optimized distribution (dotted curve).

directed to the peripheral grating region possessing low local efficiency. The difference is visible, but does not have a significant influence on instrument behavior.

The possibility for improving grating properties is worth discussing here. If the modulation distribution is changed from the measured one [Fig. 9(a), solid curve] to a more desirable one [Fig. 9(a), dotted curve], for example, by appropriate preexposure, we can get a total efficiency increase for each value of ϕ_B/ϕ_G. In Fig. 9(b), the result at 441 nm is presented. In the region $\phi_B/\phi_G > 0.5$ absolute efficiency gain amounts to 5%, which is almost the same as that for homogeneous illumination. Further attempts in this direction are technologically difficult and undesirable, and they are not likely to lead to greater efficiency. Higher total efficiencies can be attained only by changing the symmetrical groove profile into an asymmetrical one, i.e., by using blazed grooves.

An interesting concern for improving spectrometer imaging behavior has been described by Savushkin *et al.*[10] They suggest changing the blaze angles across a grating in such a way that the areas of a grating that contribute the most to image degradation have the lowest efficiency and vice versa. The grating of this paper fulfills this suggestion quite well, although admittedly by accident.

CONCLUSIONS

A concave holographic sinusoidal grating is investigated in the visible spectral region from a local and integral efficiency point of view.

Complete local efficiency maps are measured at 10 wavelengths. Experimentally evaluated groove-depth distribution gives the opportunity for theoretical calculation of these maps. The coincidence between measurements and numerical results is good even though the grating is not shallow.

Integral efficiency is calculated by a weighted summation of local efficiencies that enables us to analyze the influence of divergence and transversal intensity distribution of the illuminating Gaussian beam. Spectral dependence of total efficiency is measured and agrees well with numerical predictions. Anomalies in the spectral behavior tend to decrease when the illuminated part of the grating surface increases. Anomalies in efficiency maps are not expressed in integral spectral behavior of the grating, but they can explain its important peculiarities (polarization effects, influence of beam divergence, and distribution). These anomalies are connected with nonuniformity of modulation depth across the grating area and with relatively high values of wavelength-to-period ratio λ/d.

REFERENCES

1. M. C. Hutley, *Diffraction Gratings* (Academic, New York, 1982), Chap. 7, pp. 215–262.
2. E. G. Loewen, "Diffraction gratings, ruled and holographic," in *Applied Optics and Optical Engineering*, G. A. Vanasse, ed. (Academic, New York, 1983), Vol. IX, Chap. 2, pp. 33–71.
3. T. Namioka, M. Seya, and H. Noda, "Design and performance of holographic concave gratings," Jpn. J. Appl. Phys. **15**, 1181–1197 (1976).
4. W. R. Hunter, "Diffraction gratings for the vacuum ultraviolet spectral region," Nucl. Instrum. Methods **172**, 259–268 (1980).
5. M. Nevière and W. R. Hunter, "Analysis of the changes in efficiency across the ruled area of a concave diffraction grating," Appl. Opt. **19**, 2059–2065 (1980).
6. W. R. Hunter, in *Spectrometric Techniques*, R. R. Shannon and J. C. Wyant, eds. (Academic, New York, 1985), Vol. IV, Chap. 2, pp. 63–180.
7. R. Petit, ed., *Electromagnetic Theory of Gratings—Topics in Current Physics* (Springer-Verlag, Heidelberg, 1980), Vol. 22.
8. E. Popov and L. Mashev, "Conical diffraction mounting generalization of a rigorous differential method," J. Opt. (Paris) **17**, 175–180 (1986).
9. E. G. Loewen and M. Nevière, "Simple selection rules for VUV and XUV diffraction gratings," Appl. Opt. **17**, 1087–1092 (1978).
10. A. V. Savushkin, E. A. Sokelava, and G. P. Startsev, "Optimization of the spectral and energy characteristics of concave diffraction gratings," Sov. J. Opt. Technol. **54**, 376–378 (1987).